ELSEVIER

Cardiovascular Research 70 (2006) 543 – 554

Cardiovascular Research

www.elsevier.com/locate/cardiores

Inhibition of basic leucine zipper transcription is a major mediator of atrial dilatation

Izhak Kehat [a,b], Ronit Heinrich [b], Ofer Ben-Izhak [c], Hiroshi Miyazaki [d], J. Silvio Gutkind [e], Ami Aronheim [b,*]

[a] Department of Internal Medicine C and Cardiology, Rambam Medical Center, Haifa, Israel
[b] Department of Molecular Genetics, The B. Rappaport Faculty of Medicine, Technion-Israel Institute of Technology, 7 Efron St., Bat-Galim, Haifa 31096, Israel
[c] Department of Pathology, Rambam Medical Center, Israel
[d] Philips Institute of Oral and Craniofacial Molecular Biology, Richmond, VA, USA
[e] Oral and Pharyngeal Cancer Branch, National Institute of Dental Research, National Institute of Health, Bethesda, MD, USA

Received 25 August 2005; received in revised form 5 February 2006; accepted 17 February 2006
Available online 6 March 2006
Time for primary review 33 days

Abstract

Objective: Atrial fibrillation is the most prevalent clinically significant cardiac arrhythmia. Atrial dilatation, a predictor of atrial fibrillation, is thought to result from increased ventricular pressure. However, the underlying molecular mechanisms responsible for atrial dilatation are largely unknown. Here we sought to examine whether the expression of a basic leucine zipper inhibitor protein, JDP2, in the heart is sufficient for the generation of atrial dilatation.
Methods: A tetracycline-regulated transgene was used to express JDP2 specifically in the mouse heart. Mice hearts were dissected and subjected to Northern and Western analysis, or analyzed by ECG recording and echocardiography. Regulation of gene expression was studied using electromobility shift assays and luciferase gene reporter analysis.
Results: Expression of JDP2 resulted in massive bi-atrial dilatation, defects in conduction, and a lethal phenotype. These effects were developmentally independent, acquired during adulthood, and were reversible upon abolishing of JDP2 expression. Connexin 40 and myosin light chain 2a expression were identified as potential target genes.
Conclusion: Expression of basic leucine zipper transcription inhibitors is sufficient to results in atrial dilatation. This dilatation is acquired postnatally and is reversible. Thus, basic leucine zipper transcription inhibitors may be a relevant therapeutic target for preventing atrial dilatation and atrial fibrillation.

Keywords: Trial function; Hypertrophy; Connexins; Gene expression

1. Introduction

Atrial fibrillation (AF) is the most prevalent clinically significant cardiac arrhythmia. Its occurrence is associated with a sevenfold increased risk of stroke and a twofold increase in mortality [1,2]. Numerous studies have shown a marked correlation between atrial dilatation and the development of AF [3,4]. Whereas the cause of ventricular hypertrophy and the signaling components, from membrane-bound receptors to nuclear transcription factors, are well established [5], the pathways involved in atrial dilatation are largely unknown.

Accumulating evidence suggests that nuclear transcription factors from the basic leucine zipper (bZIP) family play an important role in cardiac development and function. This class includes the CREB/ATF family of transcription

* Corresponding author. Tel.: +972 4 8295226; fax: +972 4 8295225.
E-mail address: aronheim@tx.technion.ac.il (A. Aronheim).

0008-6363/$ - see front matter © 2006 European Society of Cardiology. Published by Elsevier B.V. All rights reserved.
doi:10.1016/j.cardiores.2006.02.018

factors, namely CREB, CREM (cAMP response element modulator), ATF, and the related AP-1 and C/EBP families. Members of the bZIP protein family can either homodimerize or heterodimerize and bind CRE or the closely related TPA response element (TRE) DNA motifs at variable efficiency [6,7]. Combinatorial interactions among different bZIP proteins have distinct effects on gene transcription [8,9].

Since the CRE and TRE DNA motifs appear in numerous promoters [10], including those of many cardiac specific genes, an effort has been made to elucidate the role of specific bZIP members in the heart. Unfortunately, little insight could be gained from knockout experiments either because of embryonic lethal phenotypes or because of functional compensation by other bZIP family members [11–13]. Consequently, transgenic models with overexpression of native or mutant bZIP proteins were developed. Surprisingly, cardiac overexpression of several inhibitory transcription factors from the bZIP family (further designated as: inhibitory bZIP proteins), such as a non-phosphorylatable form of CREB ($CREB_{ser133}$) [14], a non-functional isoform of CREM [15], or ATF3 [16] resulted in massive atrial dilatation. The overexpression of inactive bZIP proteins can displace either endogenous activating or inhibitory factors. In addition, ATF3 can function either as a transcriptional repressor or activator [8,9,17]. Thus, the precise role of transcriptional inhibition or activation responsible for atrial dilatation in these models could not be ascertained [16].

Another difficulty in interpreting the atrial phenotype in the above-mentioned models stemmed from the use of the α-myosin heavy chain (α-MHC) promoter to direct the cardiac transgene expression [14–16]. The α-MHC promoter was reported to be active in the atria on embryonic day 10, whereas in the ventricles the promoter becomes active only 12 h before birth [18]. Hence, it was postulated that atrial dilatation resulted from the selective early expression of the transgene in the atria [16], and thus represented a secondary developmental event [14,16].

c-Jun dimerization protein 2 (JDP2) is a potent inhibitory bZIP protein that can form a stable homodimer as well as a heterodimer with Jun family members and ATF2; it binds DNA, and represses transcription by multiple mechanisms [19,20]. JDP2 exhibits a 47% identity overall with ATF3 and up to 90% similarity within the bZIP motif. However, unlike ATF3, which is an immediate early gene, JDP2 is constitutively expressed, albeit in low levels, in all cell lines and tissues tested. In addition, whereas ATF3 is able to activate/repress transcription, depending on its dimerization state [8,21,22], JDP2 represses transcription either as a homo- or hetero-dimer [19,20].

To determine whether the bZIP inhibition of transcription is a primary event sufficient to cause atrial dilatation, we overexpressed JDP2 in the mouse heart in a temporally controlled manner. Indeed, the expression of JDP2 was sufficient for the development of bi-atrial dilatation and a lethal phenotype. These effects were developmentally independent and reversible.

2. Materials and methods

2.1. Generation of transgenic mice

The hemagglutinin (HA) epitope-tagged JDP2 cDNA was inserted into the bi-cistronic pBI-G expression plasmid (Clontech Inc.). The tet-promoter is designed to drive bi-directionally the β-galactosidase gene and HA-JDP2. Following injection of the linearized plasmid into oocytes, seven germ line transmitting mouse lines with a variable number of JDP2 integration copies were obtained. One of the lines containing 9 tandem copies was crossed with a α-MHC-tTA driver line (kindly provided by Prof. E. Keshet) to direct expression in the heart [23]. Genotyping was performed by PCR on genomic mice tail DNA extracted using the Redextract-*N*-AMP tissue PCR kit (Sigma, St. Luis, MO, USA).

JDP2 forward primer ATGATGCCTGGGCAGATCCCA
JDP2 reverse primer TCACTTCTTGTCCAGCTGCTCC
Tet forward primer GCTGCTTAATGAGGTCGGAATCG
Tet reverse primer GCCCCACAGCGCTGAGTGCAT

2.2. Western blot analysis

Whole cell extracts were prepared and collected as previously described [24]. For protein extraction atria were micro-dissected from the ventricles and processed apart. The following primary polyclonal antibodies were used: anti-ATF3, anti-Cx40, anti-Cx43 (all from Santa Cruz Biotechnology), and anti-Cx45 (Chemicon), anti-MLC2a (a kind gift of Dr. Ju Chen) [25] and anti-JDP2 [20]. Anti-tubulin monoclonal antibody (Sigma) was used for protein loading control. Bound antibodies were detected using enhanced chemiluminescence reagent (Amersham Inc.) according to the manufacturers' instructions, and visualized by autoradiography.

For β-galactosidase activity assay 1 μg of tissue was used and activity was determined as the absorbance at 420 nm.

2.3. Electromobility shift assay (EMSA)

EMSA was performed using atrial extracts (10 μg) or purified bacterially expressed proteins (100 ng). The [γ-^{32}P]-ATP-labeled oligonucleotides and the proteins were incubated in a 20 μl total volume of binding buffer containing 20 mM HEPES (pH 7.9), 1 mM EDTA, 150 mM KCl, 4 mM $MgCl_2$, 5 mM dithiothreitol, 0.2 mg/ml poly(dI–dC), 10% glycerol. Binding reaction was performed at RT

for 30 min. The samples were resolved in 6% polyacrylamide gels with 0.5 TBE as running buffer.

Sequence of oligonucleotides used in this study:

Jun–TRE
TTCGGGGTGACATCATGGGCT
GCCCCACTGTAGTACCCGATA
CRE
TCGATTGGCTGACGTCAGAGAG
CTAACCGACTGCAGTCTCTCTC
CRE CONNEXIN 40
GATCGACAGTGACGGCGGAGAG
CTGTCACTGCCGCCTCTCCTAG
TRE CONNEXIN 40
GATCTGAGCAACTGAGTCACCACG
ACTCGTTGACTCAGTGGTGCCTAG

2.4. Histology

Specimens were cryo-sectioned and stained with anti-Cx40 antibodies 1:200 (Chemicon), anti-Cx43 antibodies 1:200 (Santa Cruz), anti-JDP2, and anti-sarcomeric-α-actinin 1:400 (Sigma) antibodies. Nuclei were counter-stained using To-Pro3 (Molecular Probes Inc.). For cell size analysis sections were stained with wheat germ agglutinin–tetrarhodamine isothiocyanate (TRITC) (50 μg/mL) (Sigma).

2.5. Northern blot analysis

Atria and ventricles from five mice were pooled, and RNA was extracted using the RNeasy Fibrous tissue kit (Qiagen Inc.). RNA was immobilized to Hybond-*N* membrane. Hybridization with oligonucleotide probes at 37 °C in ExpressHyb hybridization solution (Clontech Inc.). The following oligonucleotides was used:

ANF: CCGGAAGCTGTTGCAGCCTAGTCCACTC-TGGGCTCCAATCCTGTCAATCCTACCCCC-GAAGCAGCTGGA-3′,
α-MHC: CGAACGTTTATGTTTATTGTGGATTGGCC-ACAGCGAGGGTCTGCTGGAGAGGT-TATTCCTCGTC-3′;
β-MHC: GAGGGCTTCACGGGCACCCTTA-GAGCTGGGTAGCACAAGATCTACTCCT-CATTCAGGCC-3′;
α-skeletal actin: TGGAGCAAAACAGAATGGCTGGCT-TTAATGCTTCAAGTTTTCCATTTCC-TTTCCACAGGG-3′;
MLC2v: CACAGCCCTGGGATGGAGAGTGGGCTGT-GGGTCACCTGAGGCTGTGGTTCAG-3′;
MLC2a: GAGGTGACCTCAGCCTGTCTACTCCT-CTTTCTCATCCCCG-3′
c-Jun: GCGATCGGGCTCTGCCGCCCGGCCTCCAA-CAACTGTCCCCTCCTCCGCTGTGAGGGG-GAG-3′
28S: AACGATCAGAGTAGTGGTATTTCACC-3′.

2.6. Luciferase assay

Transfections were performed with X-tremeGENE transfection reagent (Roche Molecular Biochemicals). HeLa cells were transfected with plasmid DNA mixture composed of the Cx40–luciferase reporter plasmid (−1190 to +121 promoter fragment, kind gift of Prof. E. Beyer) or the MLC2a-luciferase reporter plasmid (−4237 to −3478), and either an expression plasmid encoding for JDP2, ATF3 (kind gift of Prof. T. Hai), and/or c-Jun. Total protein lysates were prepared and used to measure luciferase activity (Promega Inc.).

2.7. ECG recordings

Mice were lightly anesthetized with a mixture of ketamine (125 mg/kg) and xylazine (12.5 mg/kg) by subcutaneous injection. Standard three lead ECG was recorded using 3 tungsten-coated needle electrodes (EL450) and an MP-100 acquisition system with AcqKnowledge 3.7.3Software, all from BIOPAC systems, Inc. (Santa Barbara, CA, USA).

2.8. Echocardiography

Mice (4 weeks old) were anesthetized with 1% isoflurane and kept warm at 37 °C. Echocardiography was performed using a General-Electric Vivid ultrasound imaging system equipped with a 10-MHz array transducer. Conventional two-dimensional imaging and M-Mode recordings were performed to determine cardiac size and shape. All values were based on the average of at least three measurements.

2.9. Animal studies

The investigation conforms with the *Guide for the Care and use of Laboratory Animals* published by the US National Institute of Health (NIH Publication No. 85-23, revised 1996). Institutional approved application No. IL-82-10-2003.

Angiotensin II (2 μg/kg, 100 μg/kg, Sigma Chemicals Ltd.), or 0.9% NaCl was injected intraperitoneally. Briefly, mice were anesthetized and the atria and ventricles were harvested after 1 h, 8 h or 2 days. Atria or ventricles from 3 mice in each group were pooled for protein extracts.

2.10. Statistics

A two-tailed Student's *t* test was used to compare continuous variables. $p < 0.05$ was considered significant.

3. Results

3.1. JDP2 and ATF3 DNA binding

Different bZIP family members bind the CRE and TRE DNA target sites with variable affinities. Since

JDP2 exhibits 90% similarity within the bZIP domain with ATF3 [20], we initially examined the DNA binding specificity of JDP2 and ATF3, using an in vitro electromobility shift assay (EMSA). Briefly, purified recombinant JDP2 and ATF3 proteins were incubated with labeled TRE oligonucleotides in the absence or presence of different concentrations of competing non-labeled CRE or TRE oligonucleotides (Fig. 1A). This analysis showed that the binding of JDP2 and ATF3 to the CRE and TRE motifs is similar. However, whereas ATF3 can either activate or repress transcription [8], JDP2 inhibits transcription either as a hetero- or homo-dimer. Thus, to assess the effect of bZIP transcription inhibition to mice heart function, we used JDP2 over-expression in the heart.

3.2. Generation of transgenic mice

The hemagglutinin (HA) epitope-tagged JDP2 cDNA was inserted into a bi-cistronic expression plasmid containing the tet-promoter. This plasmid directs the expression of both JDP2 and the β-galactosidase reporter under the control of the tetracycline regulator. A corresponding mouse line showing germ line transmission was crossed with a driver mouse line expressing the tetracycline activator under the control of the α-MHC promoter [23], representing the 'tet-off' system [26]. The double transgenic mice (Tet-JDP2/α-MHC-tTA) expressing JDP2 exclusively in the heart are referred as JDP2-transgenics.

JDP2-transgenic mice exhibited high cardio-specific expression of the JDP2 transgene, as assessed by the β-galactosidase reporter activity and by JDP2 protein levels. Transgene expression levels were comparable in the ventricle and the atria (Fig. 1B and C). Immuno-fluorescence showed specific nuclear and peri-nuclear JDP2-staining of cardiomyocytes (Fig. 1D).

3.3. Atrial dilatation in JDP2-transgenic mice

JDP2-transgenic mice were born at the expected ratio with no overt phenotype. However, 4-week-old mice

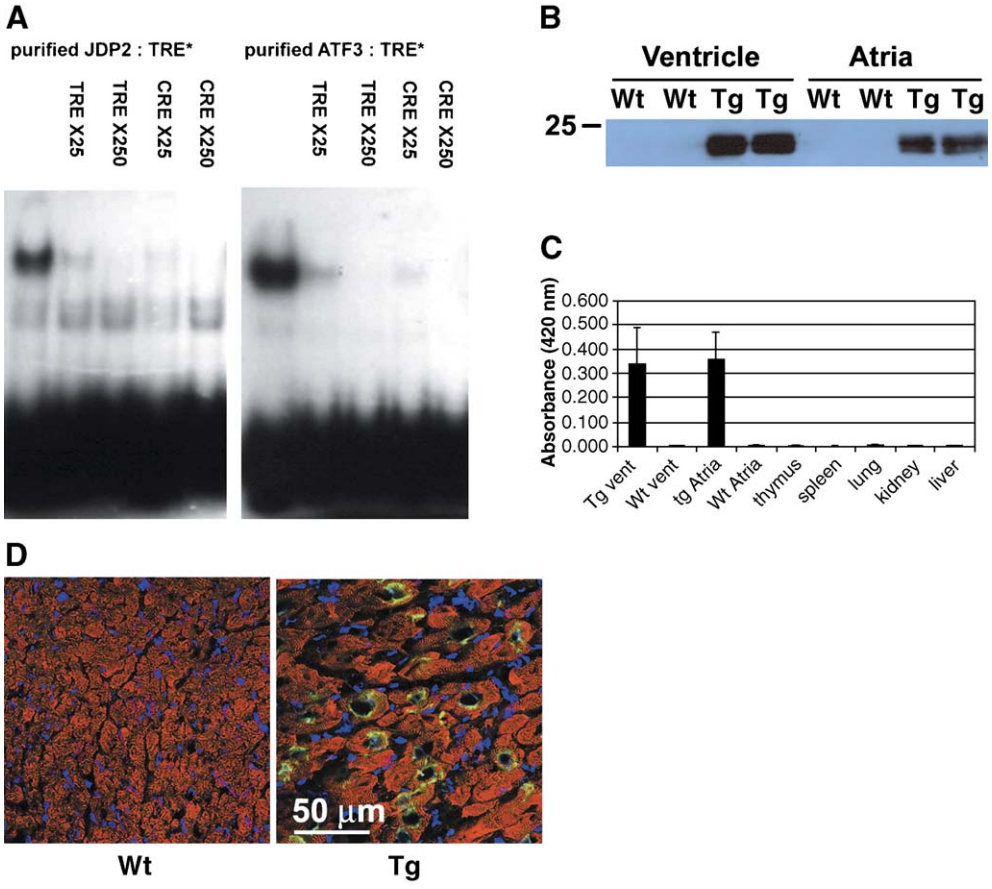

Fig. 1. JDP2 and ATF3 have similar DNA binding specificities and similar cardio-specific expression of JDP2 in the transgenic mice model. (A) EMSA, with Jun–TRE as a DNA probe, along with recombinant purified His-JDP2 and His-ATF3 (100 ng), were used for the binding reaction. Non-labeled competitive CRE and TRE DNA elements were used at a 25- and 250-fold excess where indicated. (B) Western blot analysis with anti-JDP2 antibodies and total cell lysate derived from ventricles and atria of JDP2-transgenic animals (Tg) as compared with wild-type animals (Wt). (C) Quantitative β-galactosidase reporter activity of atrial and ventricle lysate derived from either wild-type or JDP2-transgenic animals, of the indicated tissues. (D) Immunofluorescence of atrial sections stained with anti-JDP2 antibody (green), anti-sarcomeric α-actinin antibody (red), and nuclei (blue). Sections of wild-type mouse shown at the top (Wt) and a JDP2-transgenic mouse shown at the bottom (Tg).

exhibited a high rate of mortality (22% vs. 0% in JDP2-transgenic vs. wild-type mice). At this age, the JDP2-transgenic mice displayed massive atrial dilatation with a slight ventricular hypertrophy (Fig. 2A), with chambers weight of 8.1 and 1.1 times the weight of wild-type animals, respectively (Fig. 2B). No significant change in body weight or lung/body weight ratio was observed between the wild-type and JDP2-transgenic mice, indicating no increase in systemic or pulmonary pressure and edema. Heart sections showed massive bi-atrial dilatation with increased trabeculation in JDP2-transgenic mice, without apparent hypertrophy of chamber walls (Fig. 2C). Histological sections revealed hypertrophic cardiomyocytes in the atria (Fig. 2D), without fibrosis on mason-trichrome staining (data not shown). Cell size was assessed following staining of histological sections with TRIC-labeled wheat germ agglutinin. This analysis showed a significant increase in atrial, but not ventricular, myofibrillar cross-sectional diameter (Fig. 2E and F). Sections also displayed karyomegaly and abnormally shaped nuclei. Functional analysis using echocardiography revealed no difference between wild-type and JDP2-transgenic mice in ventricular wall dimensions, chamber size and ventricular fractional shortening (Table 1). Additional analysis showed no difference even following isoproterenol administration (not shown). Collectively, these data suggest that atrial dilatation represents a primary event and did not result from increased ventric-

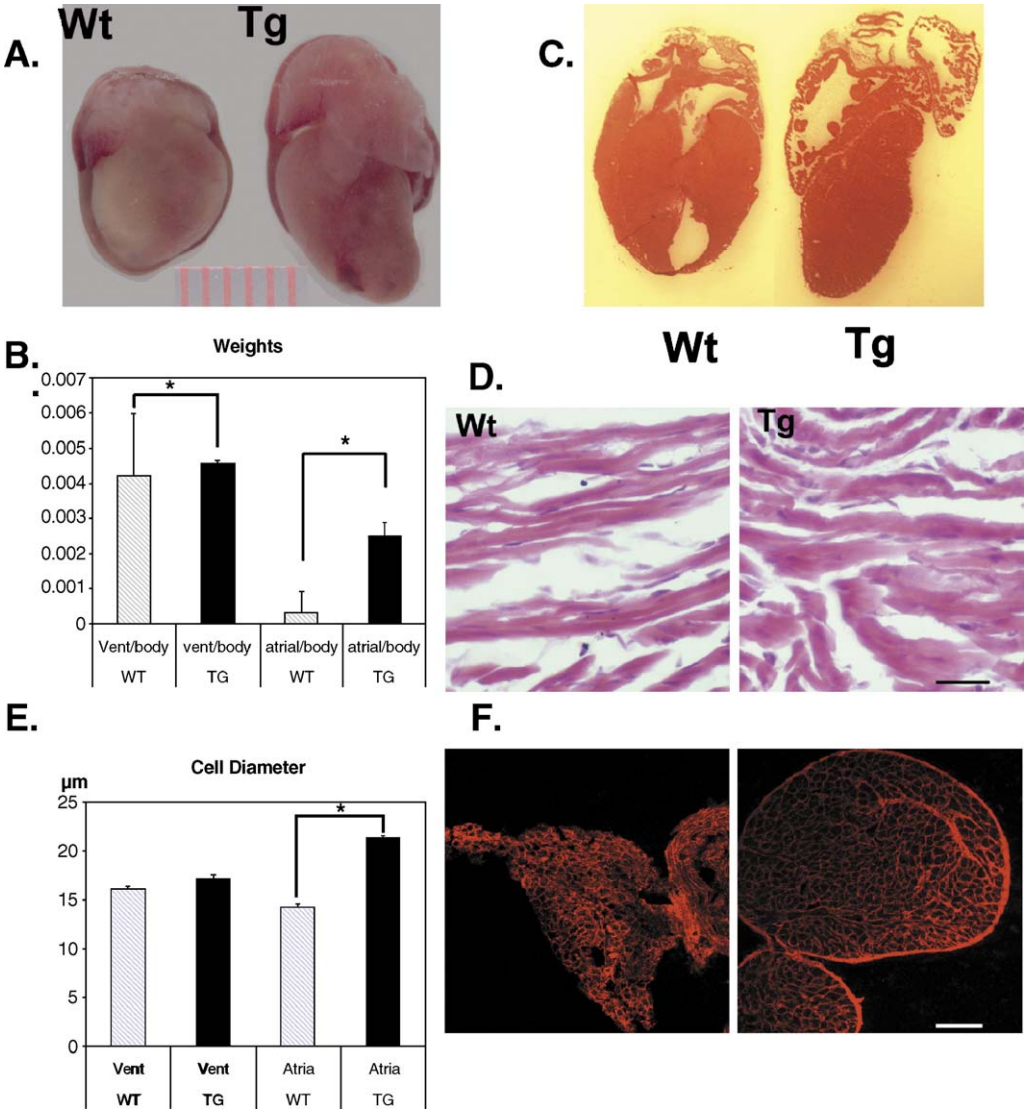

Fig. 2. JDP2 transgenic animals display massive bi-atrial dilatation and hypertrophy. (A) Micrograph of 4-week-old wild-type (Wt, left) and JDP2-transgenic (Tg, right) mice. (B) Analysis of ventricular and atrial weight normalized to body weight ($n=8$, *$p<0.05$). (C) Section of perfused fixed heart derived from wild-type (left) and transgenic animals (right). (D) High magnification (×40) hematoxylin and eosin staining of atrial sections derived from wild-type and JDP2-transgenic hearts. Scale bar=100 µm. (E) Cell cross-sectional diameter was measured in sections following wheat-germ agglutinin staining showing a significant increase in atrial, but not ventricular cell size ($n=4$ mice, 300 cells, *$p<0.05$). (F) Wheat-germ agglutinin staining of atrial sections derived from wild-type and JDP2-transgenic hearts. Scale bar=100 µm.

Table 1
Echocardiographic analysis of wild-type and JDP2-transgenic mice

	Wild-type	JDP2-transgenic	*P* value
LVD_{ed} (mm)	2.66±0.31	2.94±0.14	NS
LVD_{es} (mm)	1.44±0.22	1.58±0.13	NS
IVS_d (mm)	0.78±0.0004	0.75±0.008	NS
PW_d (mm)	0.79±0.005	0.78±0.009	NS
LV %FS	46.4±2.3	46.0±5.2	NS

Values are means±S.E.M.; $n=7$ mice. LVD_{ed}=left ventricular dimension at end diastole. LVD_{es}=left ventricular dimension at end systole. IVS_d=interventricular septum dimension (diastolic). PW_d=posterior wall dimension (diastolic). LV %FS=fractional shortening. NS=not significant.

ular pressure. The phenotype observed is very similar to the phenotype obtained in mice with ATF3 cardiac overexpression [16].

3.4. Conduction defects and sudden death in JDP2-transgenic mice

To explore the possible causes of death, we recorded the ECG in 4-week-old mice. These recordings revealed giant P waves in JDP2-transgenic mice, indicating massive atrial dilatation (Fig. 3A). Atrial and atrioventricular conduction time (PR interval) was almost double in JDP2-transgenic mice compared with controls (0.069±0.016 vs. 0.036±0.018 sec, $p<0.001$, $n=7$). JDP2-transgenic mice also had slightly faster heart rates compared with wild-type controls (274±62 vs. 201±33 bpm, respectively $p<0.001$, $n=7$). The cause for this increased rate was not determined. Some animals displayed atrioventricular conduction block and Wenckebach periodicity, whereas others exhibited this

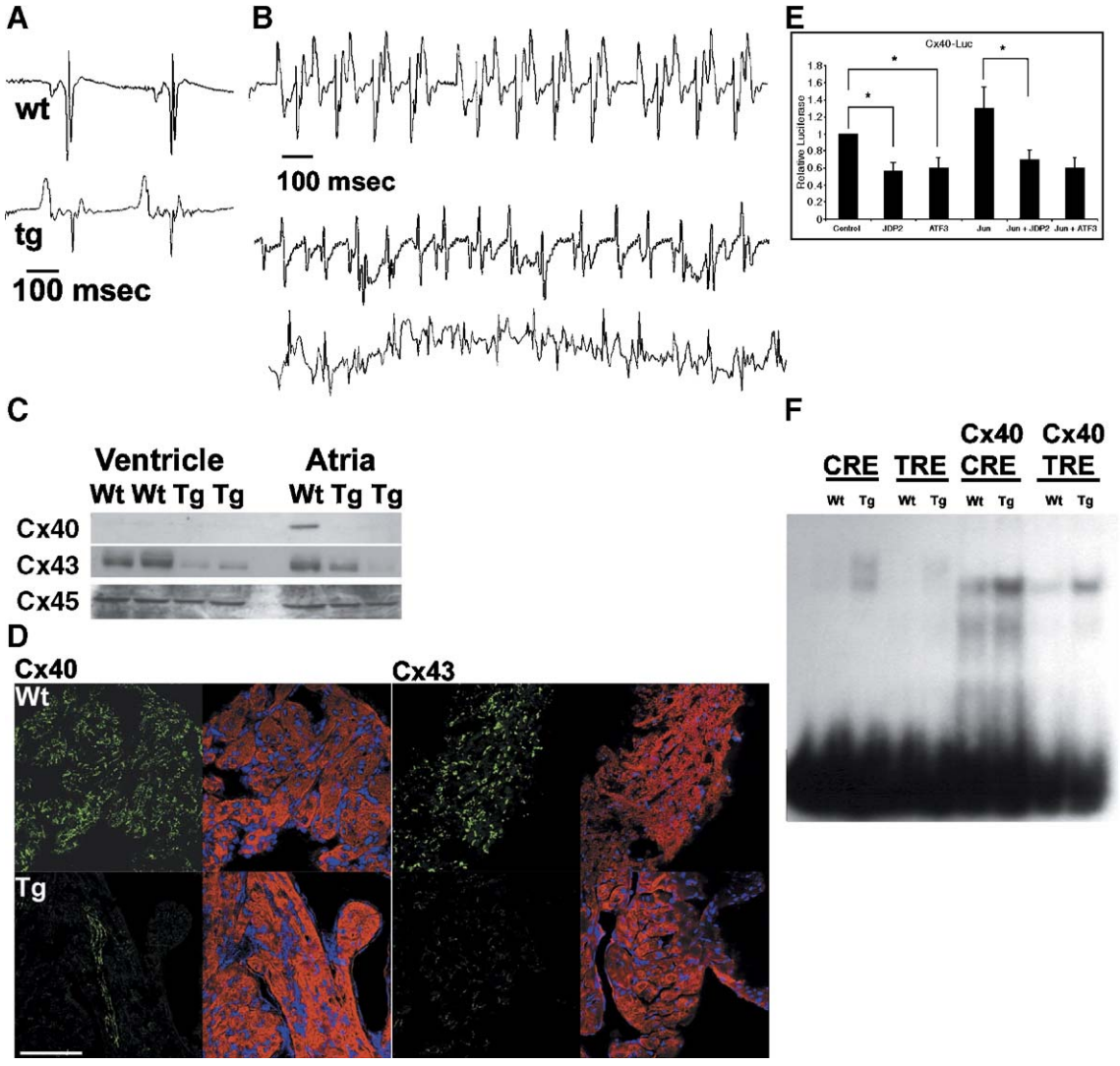

Fig. 3. Conduction defects and loss of Cx40 expression in JDP2-transgenic mice. (A) ECG recording from 4-week-old wild-type (top) and JDP2-transgenic mice (bottom). (B) Continuous ECG recording from a transgenic animal showing: Wenkebach atrioventricular block (top), atrioventricular dissociation (middle), and atrial fibrillation (bottom). (C) Western blot analysis with anti-Cx40 (top), anti-Cx43 (middle), and anti-Cx45 (bottom) antibodies of ventricle and atria lysate derived from wild-type and JDP2-transgenic mice. **(D)** Confocal immuno-fluorescence image of wild-type (top) and JDP2-transgenic (bottom) atria stained for Cx40 or Cx43 (green), sarcomeric α actinin (red), and nuclei (blue). (E) Cx40–luciferase reporter assay in HeLa cells co-transfected with the indicated expression plasmids. Mean±S.E.M., $n=5$, $^*p<0.05$. (F) EMSA with labeled CRE, Jun–TRE, Cx40–CRE, and Cx40–TRE as DNA probes and total atrial lysate from wild-type (Wt) and JDP2-transgenic mice (Tg).

phenomenon only following isoproterenol stimulation (Fig. 3B, top). A few mice developed more advanced defects such as atrioventricular dissociation (Fig. 3B, middle), and we could also document spontaneous AF (Fig. 3B, bottom). No ventricular ectopic activity or arrhythmia was observed, even after isoproterenol administration. These data suggest that the animals probably died because of fatal bradyarrhythmia and an atrioventricular block.

Because conduction in the heart is dependent on the presence of the gap junction proteins, namely connexins, the expression of these proteins was analyzed by Western blotting. In mammals, connexin 40 (Cx40) is strongly co-expressed with connexin 43 (Cx43) in the atria and is absent from the ventricular working myocardium [27]. Importantly, the JDP2-transgenic animals showed markedly lower expression of the atrial isoform Cx40 and of Cx43 (Fig. 3C). Moreover, immuno-fluorescence of heart sections revealed that Cx40 and Cx43 expression was highly suppressed in cardiomyocytes derived from JDP2-transgenic as compared with wild-type mice (Fig. 3D). Notably, the neighboring endothelial cells in the JDP2-expressing heart exhibited normal Cx40 staining. This indicates that Cx40 down-regulation is directly transgene-dependent. Down-regulation of Cx43 was less pronounced then that of Cx40. The level of connexin 45 (Cx45) remained unchanged (Fig. 3C). To further test whether the down-regulation of Cx40 was a direct result of bZIP inhibition, we co-transfected HeLa cells with Cx40–luciferase reporter plasmid (−1190–+121) [28] in the absence or presence of bZIP repressors, either with ATF3 or JDP2 alone or together with c-Jun. Whereas c-Jun slightly up-regulated the Cx40 promoter, both ATF3 and JDP2 expression resulted in marked suppression of the Cx40-dependent luciferase activity (Fig. 3E). The Cx40 promoter contains both CRE-like (TGACG) and TRE-like (TGAGTCA) motifs. EMSA analysis with total cell lysate derived from JDP2-transgenic mice atria revealed enhanced DNA binding activity for the general CRE and TRE, as well as for the CRE and TRE DNA elements derived from the Cx40 promoter (Fig. 3F). Expression analysis showed down-regulation of Cx40 and Cx43, but not Cx45 message in JDP2-transgenics (Fig. 4A). Thus we conclude that JDP2 is able to bind the CRE binding sequences located at the Cx40 promoter and results in transcription inhibition.

3.5. Gene expression in JDP2-transgenic mice

Although only mild hypertrophy was noted in the ventricles of JDP2-transgenic mice, gene expression analysis revealed the typical reactivation of fetal genes such as: β-MHC, α-skeletal-actin, and atrial natriuretic factor (ANF) in the ventricles (Fig. 4A). The mRNA level of the myosin light chain regulatory protein MLC2 ventricular isoform, MLC2v, was slightly elevated in the ventricles of JDP2-transgenics. In contrast, in the atria, the mRNA of the myosin light chain isoform, MLC2a, was markedly down-regulated (Fig. 4A). Interestingly, the c-Jun mRNA level did not show an appreciable change. A pronounced reduction of the α-MHC mRNA levels was observed in the ventricles of JDP2-transgenic mice compared with the atria. Despite the fact that the JDP2 transgene expression is dependent on the activity of the α-MHC promoter, the JDP2 expression level

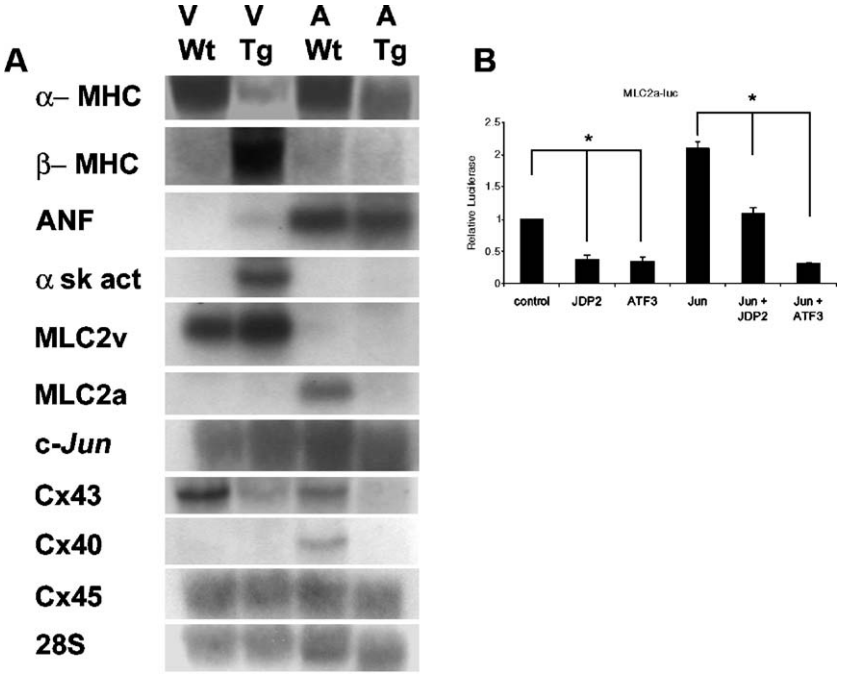

Fig. 4. Gene expression analysis of JDP2-transgenic and wild-type mice. (A) Analysis by Northern blotting. The mRNA levels of the indicated transcripts are shown. Total mRNA derived from ventricles (V) and atria (A) of wild-type (Wt) and JDP2-transgenic (Tg). The 28S RNA serves as a loading control. (B) MLC2a-luciferase reporter assay in HeLa cells co-transfected with the indicated expression plasmids. Mean±S.E.M. $n=5$, $^{*}p<0.05$.

in the ventricle was not affected and was comparable to the expression found in the atria (Fig. 1B). This is probably because the α-MHC promoter fragment (2.9 kb) used to generate the MHC-tTA transgene is not affected by ventricular hypertrophy, as opposed to the endogenous promoter.

The very proximal MLC2a promoter does not contain CRE or TRE sites, however, a putative CRE (TTACGTCA) and TRE (TGACTCA) sites are located at distal promoter region. To further test whether the down-regulation of MLC2a was a direct result of bZIP inhibition, we co-transfected HeLa cells with MLC2a-luciferase reporter plasmid containing these putative sites (−4237 to −3478) in the absence or presence of bZIP repressors, either with ATF3 or JDP2 alone or together with c-Jun. Whereas c-Jun resulted in a twofold activation of the MLC2a promoter, both ATF3 and JDP2 expression resulted in a marked suppression of the MLC2a-dependent luciferase activity (Fig. 4B). These results suggest that both ATF3 and JDP2 are responsible for MLC2a gene down-regulation.

3.6. Atrial dilatation results from postnatal bZIP repression and is reversible

The α-MHC promoter was reported to be active in the atria on embryonic day 10, whereas in the ventricles the promoter becomes active shortly before birth [18]. To examine whether the pronounced atrial effect was due to developmental differences in the activity of the α-MHC promoter, we took advantage of the ability to regulate the binding activity of the tetracycline activator by the use of doxycycline. We initially tested the leakiness of the system in mice fed with a regular diet and in mice fed with doxycycline from mating to 8 days after birth. Interestingly, we observed no JDP2-transgene expression in the doxycycline-fed JDP2-transgenic animals' hearts either immediate-

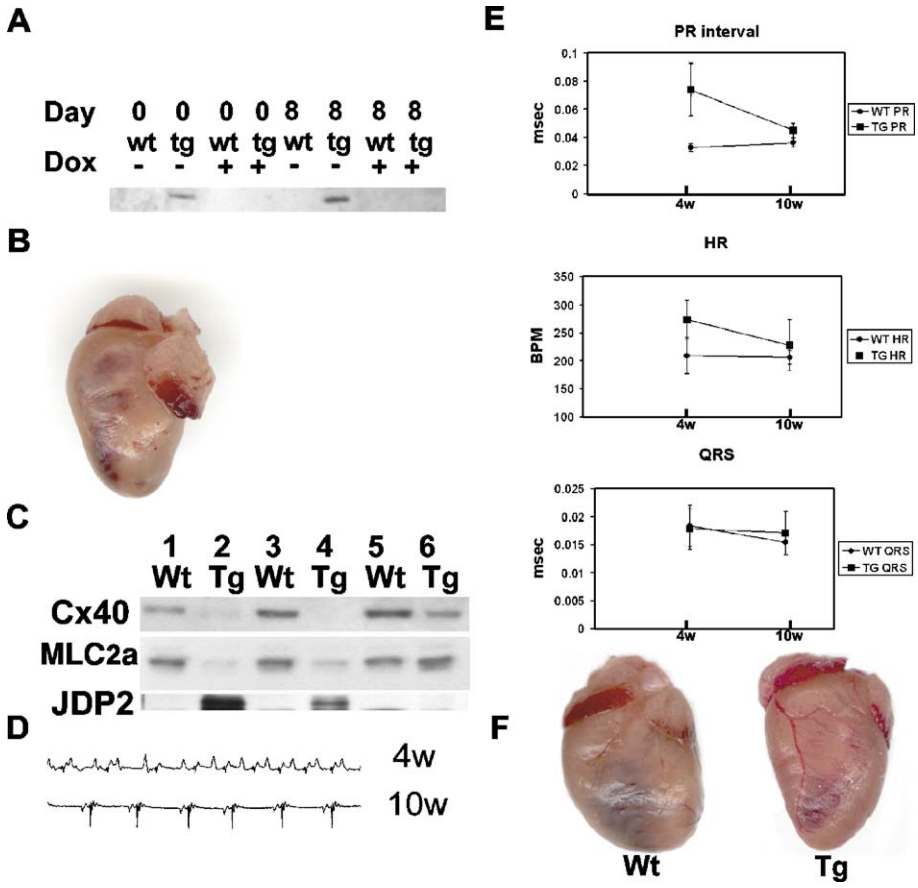

Fig. 5. Atrial phenotype of JDP2-trangenic mice is developmentally independent and reversible. (A) Analysis of JDP2 protein levels in newborn and 8-day-old pups of JDP2-transgenic (Tg) or wild-type (Wt) animals fed either without or with doxycycline from mating. (B) Representative micrograph of a 6-week-old JDP2-transgenic mouse is shown. Doxycycline was added to the mouse diet, after mating until 1 week after birth. Mice were sacrificed 5 weeks after the termination of the doxycycline treatment. (C) Western blot analysis of atrial lysates with anti-Cx40, anti-MLC2a, and anti-JDP2 antibodies. Lysate derived from atria of wild-type (Wt) and JDP2-transgenic (Tg) mice exposed to different doxycycline treatments are shown. Lanes 1–2: no doxycycline; lanes 3 and 4: doxycycline was added after mating until 1 week old. Atria harvested at 6 weeks. Lanes 5–6: doxycycline was added from 4 to 10 weeks of age and atria was harvested at 10 weeks old. (D) ECG recording from the same JDP2-transgenic mice at 4 weeks (top) and at 10 weeks (bottom) following doxycycline treatment. (E) Summary of ECG data of mice at the age of 4 weeks and following 6 weeks of doxycycline treatment for JDP2-transgenic (■) and wild-type (●) animals ($n=4$). The average and standard deviation are shown. (F) Micrograph of 10-week-old wild-type and JDP2-transgenic mice hearts treated with doxycycline from 4 weeks of age.

ly after birth or at the age of 8 days (Fig. 5A), which indicates the tight control of transgene expression during prenatal life and milking by the doxycycline treatment. In adult mice, 2 days of doxycycline treatment is sufficient to completely abolish the transgene expression and 7 days are required for JDP2 re-expression following doxycycline treatment (data not shown).

To determine whether the JDP2 atrial effects were due to the early expression of the transgene, we added doxycycline to the diet of the mice, after mating until 1 week after birth. Five weeks following the termination of the doxycycline treatment, the JDP2-transgenic mice displayed an identical dilated atrial phenotype (Fig. 5B), with early death, and the loss of atrial Cx40 and MLC2a protein expression (Fig. 5C, lanes 3, 4)). This suggests that the observed phenotype is independent of any developmental or early postnatal events.

Next, we examined the reversibility of the phenotype. A group of JDP2-transgenic and control littermates were examined by ECG recording at 4 weeks of age, which showed the typical JDP2-transgenic phenotype (Fig. 5D and E). We then added doxycycline to their diet to abolish JDP2 expression. ECG Recordings at 10 weeks of age showed a marked shortening of the PR interval and a slowing of heart rates to wild-type levels (Fig. 5D and E). Ventricular and atrial weights of JDP2-transgenic mice were 1.0 and 1.5 times the weight of the wild-type counterparts, respectively, showing an almost complete reversibility of atrial dilatation (Fig. 5F). In addition, Cx40 and MLC2a expression returned to levels similar to those observed in the atria of wild-type animals (Fig. 5C, lanes 5, 6). Collectively, we found that bZIP inhibition is sufficient to cause atrial dilatation in mice. This phenotype is acquired and reversible.

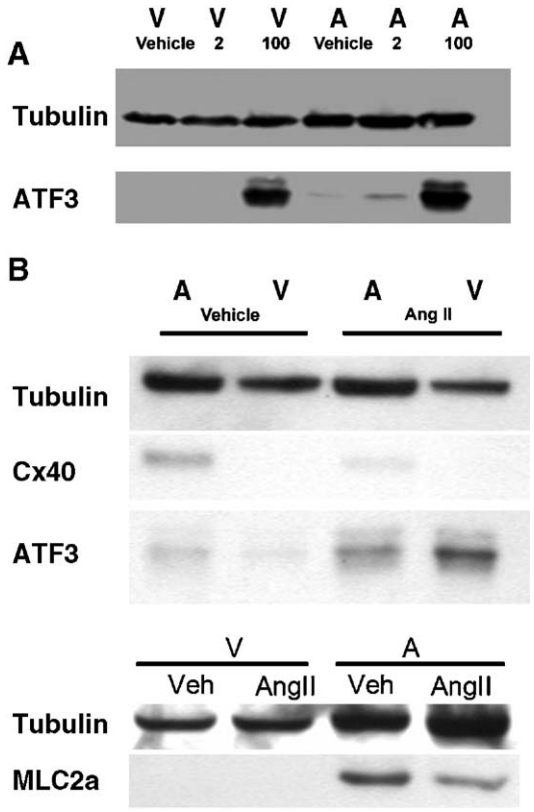

Fig. 6. Signaling pathway involved in atrial bZIP repression. (A) Western blot analysis with anti-ATF3 ventricular (V) and atrial (A) extracts 1 h after intraperitoneal injection of either 0.9% NaCl (vehicle) or angiotensin II at the indicated dose (μg/kg). Anti-tubulin served as a loading control. (B) Western blot analysis with anti-Cx40 and anti-ATF3. Top: Total cell lysate was prepared 8 h after two repeated intraperitoneal injections with a 4-h interval of vehicle or angiotensin II (AngII) 100 μg/kg. Bottom: lysate following 2 days with six repeated intraperitoneal injections with 8-h interval of vehicle or angiotensin II (AngII) 100 μg/kg. Anti-tubulin serves as a loading control.

3.7. Signaling pathway involved in atrial bZIP repression

Several studies have implicated the rennin–angiotensin pathway in the pathogenesis of AF. Therefore, we injected angiotensin II (AngII) or vehicle (0.9% NaCl) intraperitoneally to wild-type mice. One hour following injection, a significant elevation of the ATF3, but not JDP2 (not shown), protein level was observed in the atria of AngII-injected mice, but not in vehicle-injected mice (Fig. 6A). Moreover, two repeated injections of AngII resulted in a lower Cx40 protein level (Fig. 6B). Repeated injections for 2 days also resulted in down-regulation of MLC2a (Fig. 6B, bottom). Thus, AngII signaling may be involved in up-regulation of a bZIP repressor (ATF3) and down-regulation of Cx40 and MLC2a and possibly to atrial dilation and fibrillation.

4. Discussion

Our results indicate that bZIP transcriptional inhibition is sufficient to cause atrial dilatation and hypertrophy. Using ectopic expression of the potent bZIP inhibitor, JDP2, in the heart with the ‘tet-off’ binary transgenic system, we showed that this effect is independent of developmental events and is reversible.

4.1. Basic leucine zipper transcription factors

The bZIP family of proteins use a simple basic motif for DNA recognition, yet family members bind different DNA target sites with variable affinities [6]. Analysis of the basic region showed that the CRE/TRE specificity is controlled by several charged residues within the basic region [6]. JDP2 and ATF3 are identical in all of these positions; thus, it is not surprising that both JDP2 and ATF3 have similar DNA binding specificities. Since JDP2 and ATF3 bind both TRE and CRE DNA elements, we cannot determine whether inhibition of CRE, TRE, or both is responsible for the atrial dilatation observed in the JDP2 or ATF3 transgenic mice [16]. In the JDP2-transgenics, the ATF3 level was not elevated (data not shown); thus, both ATF3 and JDP2 can independently cause atrial dilatation.

4.2. JDP2-mediated atrial dilatation

Our data show that atrial dilatation, resulting from bZIP inhibitors, is an acquired postnatal phenomenon. Moreover, the structural, functional, and molecular phenotype of the JDP2-transgenic mice was almost fully reversible upon abolishing the transcriptional repression. Hence, the observed phenotype is a direct result of transgene expression, and is not due to an insertional or other non-specific effect. Overexpression of the β-galactosidase reporter gene, by itself, in the heart did not result in atrial dilatation [29]. The reversibility of the phenotype also practically rules out any congenital defect, valvular disorders, or atrial cardiomyocyte proliferation as a cause of the atrial dilatation, since these processes are irreversible. These results also suggest that atrial dilatation, similar to ventricular hypertrophy, may be therapeutically targeted, since this process may be partially reversible.

4.3. Atrial and ventricular effects of bZIP repressors

Although overexpression of repressing bZIP proteins resulted in strikingly similar massive atrial dilatation and hypertrophy, the ventricular effects were more variable. Overexpression of $CREB_{ser133}$ [14] resulted in massive ventricular dilatation and an overt heart failure with edema. The overexpression of a non-functional CREM isoform resulted in a ventricular hypertrophy without increased pressures [15]. Overexpression of ATF3 resulted in only a small increase in ventricular weight, suggesting cardiac hypertrophy, without signs of heart failure [16]. Here, JDP2 overexpression resulted in a slight (10%) increase in ventricular weight with no evidence of either systemic or pulmonary edema, strongly suggesting no increased cardiac pressures. Surprisingly, molecular markers for ventricular hypertrophy in the ventricles were observed. The α- to β-MHC switch in the JDP2-transgenic does suggest a potential ventricular derangement, which could contribute to the atrial dilatation. Nevertheless, we did not observe a reduced ventricular function. The identical atrial phenotype, along with the variable ventricular one in the different mouse models, strongly suggests that the atrial dilatation is a primary event, independent of the ventricles. Moreover, the absence of an edematous state in the JDP2, ATF3, and CREM mice practically rules out an increase in end diastolic pressures as a cause for such a massive bi-atrial dilatation. Since the CREB-dominant negative mutant, $CREB_{ser133}$, can function in multiple mechanisms [14], it is possible that bZIP inhibition has a dominant effect in the atria resulting in dilatation, whereas other, yet to be determined, independent mechanisms account for the ventricular hypertrophy.

4.4. Conduction disorders and Cx40 down-regulation

Our results showed a marked reduction in the expression of the atrial gap-junction protein, Cx40 and of Cx43. Interestingly, mice with Cx40 gene disruption also showed conduction defects and first degree atrioventricular block [30,31] similar to the one observed in JDP2-transgenic mice. Electrophysiological analysis in Cx40 knockout mice revealed a significant role for Cx40 in atrio-ventricular nodal conduction [32]. Thus, the longer atrial conduction times and the conduction blocks observed in the JDP2-transgenic mice are consistent with the down-regulation of Cx40 protein in the atria. In patients with valvular heart disease in sinus rhythm Cx40 is down-regulated in the atria [33]. However, no differences were noted in a complete atrioventricular block model of atrial dilatation [34]. These conflicting results probably result from the different mechanism of atrial dilatation and the difference in species and model.

4.5. MLC2a and atrial dilatation

Another target gene that was found to be significantly down-regulated in the atria is the MLC2 atrial isoform. Similar to Cx40, this effect was reversible upon abolishing of JDP2 expression. MLC2a disruption in mice is embryonically lethal as this is the major isoform in embryonic chamber; however, embryos display enlarged atria [25]. Overexpression of an interfering mutant, non-phosphorylatable MLC2v, in the mouse heart also caused marked bi-atrial hypertrophy and dilatation without appreciable effects in the ventricle [35]. Recently, the importance of MLC2a phosphorylation to atrial contractility was shown [36]. Collectively, these data suggest that the reduced expression of MLC2a in JDP2-expressing mice may have a causal effect in the development of atrial dilatation.

4.6. Signaling pathway involved in atrial bZIP repression

It is interesting to note that overexpression of the angiotensin converting enzyme (ACE) in the mouse heart resulted in isolated atrial dilatation and conduction abnormalities [37], and that overexpression of ACE2 resulted in conduction abnormalities, AV block, and down-regulation of Cx40 and Cx43[38]. Taken together with our results showing that injection of AngII results in up-regulation of the bZIP repressor ATF3 and down-regulation of Cx40 and MLC2a, these data suggest that the rennin–angiotensin signaling may be involved in the pathogenesis of atrial dilation.

4.7. Atrial fibrillation

Only a small minority of JDP2-transgenics developed spontaneous AF. This low rate suggests that in mice who are not prone for AF, atrial dilatation may not be sufficient for development of AF. It is also possible that the early death prevented the occurrence of AF in more animals, since in the related CREM overexpression model [15] spontaneous AF was not observed before the age of

8 weeks. In patients, the risk of developing AF increases by 39% for each 5-mm increment increase in the size of the left atria [3]. In two prospective studies, it was confirmed that atrial enlargement predicts the development of AF, and, in both cases, it was a better predictor than the presence of left ventricular hypertrophy [4,39]. These data suggest that atrial dilatation serves as a potential therapeutic target for the prevention of AF.

5. Conclusions

Atrial fibrillation is one of two emerging cardiovascular epidemics worldwide [1]. Therefore, any therapy that reduces AF in high-risk populations is likely to have a significant impact on the allocation of resources. The results of this study suggest that bZIP inhibition is sufficient to cause atrial dilation, that this dilatation is acquired postnatally, and that it is reversible upon the relief of inhibition. Thus, bZIP repressors should be identified as they may serve as novel drug targets for the prevention of atrial dilatation and fibrillation. In addition, since AP-1 is implicated in tumorogensis, inhibition of bZIP proteins is considered as an anti-tumor strategy. However, the results of this study suggest that systemic bZIP inhibition may cause atrial dilatation and that the development and use of such systemic therapies should be reconsidered.

Acknowledgments

The authors wish to thank Ms. A. Cohen and Mr. R. Lavi for their excellent technical assistance, Drs. O. Shenker and I. Suss-Toby for imaging support, and Profs. T. Hai, Chen, J., E. Beyer, E. Keshet, H. Bujard for various plasmids and reagents. This work was supported by a UICC American Cancer Society International Fellowship for Beginning Investigators and by the Israel Cancer Research Foundation and The Israel Ministry of Health grant to AA.

References

[1] Braunwald E. Shattuck lecture – Cardiovascular medicine at the turn of the millennium: triumphs, concerns, and opportunities. N Engl J Med 1997;337:1360–9.
[2] Wattigney WA, Mensah GA, Croft JB. Increasing trends in hospitalization for atrial fibrillation in the United States, 1985 through 1999: implications for primary prevention. Circulation 2003;108:711–6.
[3] Kannel WB, Wolf PA, Benjamin EJ, Levy D. Prevalence, incidence, prognosis, and predisposing conditions for atrial fibrillation: population-based estimates. Am J Cardiol 1998;82:2N–9N.
[4] Psaty BM, Manolio TA, Kuller LH, Kronmal RA, Cushman M, Fried LP, et al. Incidence of and risk factors for atrial fibrillation in older adults. Circulation 1997;96:2455–61.
[5] Liang Q, Molkentin JD. Redefining the roles of p38 and JNK signaling in cardiac hypertrophy: dichotomy between cultured myocytes and animal models. J Mol Cell Cardiol 2003;35:1385–94.
[6] Montclare JK, Sloan LS, Schepartz A. Electrostatic control of half-site spacing preferences by the cyclic AMP response element-binding protein CREB. Nucleic Acids Res 2001;29:3311–9.
[7] Shaulian E, Karin M. AP-1 in cell proliferation and survival. Oncogene 2001;20:2390–400.
[8] Hsu JC, Bravo R, Taub R. Interactions among LRF-1, JunB, c-Jun, and c-Fos define a regulatory program in the G1 phase of liver regeneration. Mol Cell Biol 1992;12:4654–65.
[9] Hai T, Hartman MG. The molecular biology and nomenclature of the activating transcription factor/cAMP responsive element binding family of transcription factors: activating transcription factor proteins and homeostasis. Gene 2001;273:1–11.
[10] Mayr B, Montminy M. Transcriptional regulation by the phosphorylation-dependent factor CREB. Nat Rev Mol Cell Biol 2001; 2:599–609.
[11] Rudolph D, Tafuri A, Gass P, Hammerling GJ, Arnold B, Schutz G. Impaired fetal T cell development and perinatal lethality in mice lacking the cAMP response element binding protein. Proc Natl Acad Sci U S A 1998;95:4481–6.
[12] Eferl R, Ricci R, Kenner L, Zenz R, Davisd J-P, Rath M, et al. Liver tumor development: c-Jun antagonizes the proapoptotic activity of p53. Cell 2003;112:181–92.
[13] Hummler E, Cole TJ, Blendy JA, Ganss R, Aguzzi A, Schmid W, et al. Targeted mutation of the CREB gene: compensation within the CREB/ATF family of transcription factors. Proc Natl Acad Sci U S A 1994;91:5647–51.
[14] Fentzke RC, Korcarz CE, Lang RM, Lin H, Leiden JM. Dilated cardiomyopathy in transgenic mice expressing a dominant-negative CREB transcription factor in the heart. J Clin Invest 1998;101: 2415–26.
[15] Muller FU, Lewin G, Baba HA, Boknik P, Fabritz L, Kirchhefer U, et al. Heart-directed expression of a human cardiac isoform of cAMP-response element modulator in transgenic mice. J Biol Chem 2005;280:6906–14.
[16] Okamoto Y, Chaves A, Chen J, Kelley R, Jones K, Weed HG, et al. Transgenic mice with cardiac-specific expression of activating transcription factor 3, a stress-inducible gene, have conduction abnormalities and contractile dysfunction. Am J Pathol 2001;159: 639–50.
[17] Hsu JC, Laz T, Mohn KL, Taub R. Identification of LRF-1 a leucine zipper protein that is rapidly and highly induced in regenerating liver. Proc Natl Acad Sci U S A 1991;88:3511–5.
[18] Subramaniam A, Jones WK, Gulick J, Wert S, Neumann J, Robbins J. Tissue-specific regulation of the alpha-myosin heavy chain gene promoter in transgenic mice. J Biol Chem 1991;266:24613–20.
[19] Jin C, Ugai H, Song J, Murata T, Nili F, Sun K, et al. Identification of mouse Jun dimerization protein 2 as a novel repressor of ATF-2. FEBS Lett 2001;489:34–41.
[20] Aronheim A, Zandi E, Hennemann H, Elledge S, Karin M. Isolation of an AP-1 repressor by a novel method for detecting protein–protein interactions. Mol Cell Biol 1997;17:3094–102.
[21] Hai TW, Liu F, Coukos WJ, Green MR. Transcription factor ATF cDNA clones: an extensive family of leucine zipper proteins able to selectively form DNA-binding heterodimers. Genes Dev 1989; 3:2083–90.
[22] Liang G, Wolfgang CD, Chen BP, Chen TH, Hai T. ATF3 gene. Genomic organization, promoter, and regulation. J Biol Chem 1996;271:1695–701.
[23] Dor Y, Djonov V, Abramovitch R, Itin A, Carmeliet P, et al. Conditional switching of VEGF provides new insights into adult neovascularization and pro-angiogenic therapy. EMBO J 2002;21: 1939–47.
[24] Heinrich R, Livne E, Ben-Izhak O, Aronheim A. The c-Jun dimerization protein 2 inhibits cell transformation and acts as a tumor suppressor gene. J Biol Chem 2004;279:5708–15.
[25] Huang C, Sheikh F, Hollander M, Cai C, Becker D, Chu PH, et al. Embryonic atrial function is essential for mouse embryogenesis,

cardiac morphogenesis and angiogenesis. Development 2003;130: 6111–9.
[26] Kistner A, Gossen M, Zimmermann F, Jerecic J, Ullmer C, Lubbert H, et al. Doxycycline-mediated quantitative and tissue-specific control of gene expression in transgenic mice. Proc Natl Acad Sci U S A 1996; 93:10933–8.
[27] van Veen AA, van Rijen HV, Opthof T. Cardiac gap junction channels: modulation of expression and channel properties. Cardiovasc Res 2001;51:217–29.
[28] Seul KH, Tadros PN, Beyer EC. Mouse connexin40: gene structure and promoter analysis. Genomics 1997;46:120–6.
[29] Yu Z, Redfern CS, Fishman GI. Conditional transgene expression in the heart. Circ Res 1996;79:691–7.
[30] Simon AM, Goodenough DA, Paul DL. Mice lacking connexin40 have cardiac conduction abnormalities characteristic of atrioventricular block and bundle branch block. Curr Biol 1998;8:295–8.
[31] Bevilacqua LM, Simon AM, Maguire CT, Gehrmann J, Wakimoto H, Paul DL, et al. A targeted disruption in connexin40 leads to distinct atrioventricular conduction defects. J Interv Card Electrophysiol 2000;4:459–67.
[32] VanderBrink BA, Sellitto C, Saba S, Link MS, Zhu W, Homoud MK, et al. Connexin40-deficient mice exhibit atrioventricular nodal and infra-Hisian conduction abnormalities. J Cardiovasc Electrophysiol 2000;11:1270–6.
[33] Gaborit N, Steenman M, Lamirault G, Le Meur N, Le Bouter S, Lande G, et al. Human atrial ion channel and transporter subunit gene-expression remodeling associated with valvular heart disease and atrial fibrillation. Circulation 2005;112:471–81.
[34] Neuberger HR, Schotten U, Verheule S, Eijsbouts S, Blaauw Y, van Hunnik A, et al. Development of a substrate of atrial fibrillation during chronic atrioventricular block in the goat. Circulation 2005; 111:30–7.
[35] Sanbe A, Fewell JG, Gulick J, Osinska H, Lorenz J, Hall DG, et al. Abnormal cardiac structure and function in mice expressing non-phosphorylatable cardiac regulatory myosin light chain 2. J Biol Chem 1999;274:21085–94.
[36] Grimm M, Haas P, Willipinski-Stapelfeldt B, Zimmermann WH, Rau T, Pantel K, et al. Key role of myosin light chain (MLC) kinase-mediated MLC2a phosphorylation in the alpha 1-adrenergic positive inotropic effect in human atrium. Cardiovasc Res 2005; 65:211–20.
[37] Xiao HD, Fuchs S, Campbell DJ, Lewis W, Dudley SC Jr, Kasi VS, et al. Mice with cardiac-restricted angiotensin-converting enzyme (ACE) have atrial enlargement, cardiac arrhythmia, and sudden death. Am J Pathol 2004;165:1019–32.
[38] Donoghue M, Wakimoto H, Maguire CT, Acton S, Hales P, Stagliano N, et al. Heart block, ventricular tachycardia, and sudden death in ACE2 transgenic mice with downregulated connexins. J Mol Cell Cardiol 2003;35:1043–53.
[39] Ciaroni S, Cuenoud L, Bloch A. Clinical study to investigate the predictive parameters for the onset of atrial fibrillation in patients with essential hypertension. Am Heart J 2000;139:814–9.